




Internal Waves over the Continental Shelf of the Heracles Peninsula: Modeling and Observation

Vitalii Ivanov , T. Ya. Shul'ga , Andrei Bagaev , Tatiana Plastun ,
Alesia Medvedeva , Ludmila Verzhevskaia , and Irina Svisheva 

Marine Hydrophysical Institute, Kapitanskaya 2, 299011 Sevastopol, Russia
shulgaty@mail.ru

Abstract. The paper considers the internal waves on the shelf of the Crimean coast, their structure and dynamics at the periphery of the Black Sea basin. Manifestations of internal waves were studied by numerical experiments and by processing of remote sensing data from high-resolution data. Maps of the vertical velocity of the first three modes of internal waves on the shelf of the Crimean coast were constructed. The phase velocity of the internal waves in the deep part of the sea for the first mode at the given profiles varies from 2.6 to 5 ms^{-1} ; for the waves of the second mode— 1.1 – 2.3 ms^{-1} ; for the waves of the third mode— 0.7 – 1.4 ms^{-1} . Wavelengths detected from the satellite data had a mean value of 0.4 km . The longest waves, around 0.8 km , were observed between Sevastopol and Yevpatoria. During June, 2017 the waves of 2^{nd} and 3^{rd} modes were observed in the area of study the most frequently.

Keywords: Black Sea · Phase velocity · Dispersion relations · Mode structure · Remote sensing · Intensive internal waves · Coastal upwelling · Topographic effects

1 Introduction

The paper investigates the appearance and propagation of internal waves at the shelf of the Black Sea, near the Heracles Peninsula. This complex phenomenon was addressed in a set of papers [1–5]. In present study, we apply numerical experiments in order to investigate the dynamics of internal waves and the conditions for their development. We studied the conditions when intense internal waves appear on the periphery of the Rim Current off the shelf of the Crimean coast. For the first time, highres images of the sea surface near the Heracles Peninsula were used. They provided a unique opportunity to assess parameters of internal waves. The results allowed us to establish theoretical spatio–temporal characteristics of internal waves that correspond to shallow pycnocline.

2 Study Area

In some areas of the Crimean shelf irregularity of the coastline/bathymetry and the Rim Current passing near the shore create specific conditions for the internal waves generation (see Fig. 1). One of such areas is to the North of the Heracles Peninsula—in Kalamita Bay, between the cities of Sevastopol and Yevpatoria. The shelf here is wide and the isobath of 150 m is located up to 60 km away from the coastline. Another area is to the South–East of the Heracles Peninsula, between the cities of Sevastopol and Yalta. The shelf here is convex and narrow (just 30 km wide). Between these two areas the shelf is even more narrow, down to 10 or even 6 km wide.

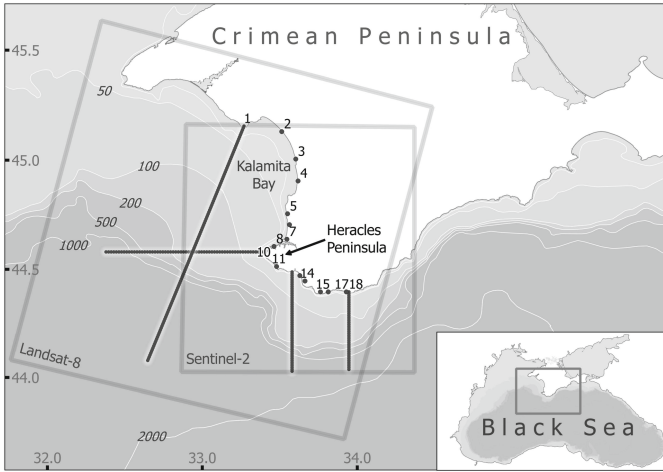


Fig. 1. The bathymetry of the Black Sea near the Crimean Peninsula. Thin white contours represent 20–, 50–, 100–, 200–, 500–, 1000–, and 2000–m isobaths. Dark-grey numbered lines depict some transects considered for the numerical experiments (for the rest only starting points and their numbers are plotted). Horizontal axis units are degrees East, vertical axis—degrees North. Light-grey rectangles outline the areas of satellite data availability. In the inset location of the area of interest is shown.

3 Methodology

In our work, we tackled the main problems stage by stage, as shown in the flowchart (Fig. 2). At the first stage, we detected and evaluated the characteristics of the surface manifestations of internal waves. At the second stage, we obtained theoretical estimates of the internal wave parameters based on the development and implementation of the algorithm for solving the full boundary value problem [6]. At the final stage, the results of theoretical and numerical studies were compared with the data obtained by remote sensing methods.

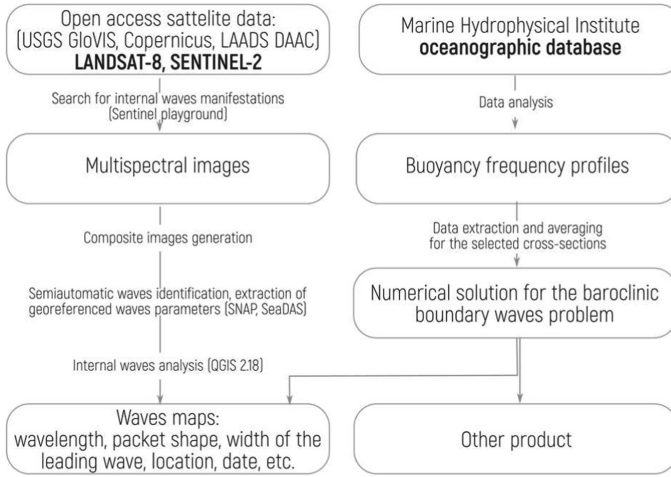


Fig. 2. Schematic flowchart of the major steps in deriving the results of the present study.

4 Data and Methods

4.1 Deriving Vertical Density Structure

Decadal temperature and salinity fields at standard levels (in the 0–1500 m layer) in the Black Sea were reconstructed using in-situ data and satellite measurements which had been collected from the 1950–es up to nowadays [7]. These fields were used to investigate the vertical density structure in the vicinity of the slope–shelf area at the Black Sea coast of the Crimea.

The following contact and remote sensing data on the Black Sea were used:

(A) Research Vessel measurements on temperature and salinity from 1951 to 2008 and temperature measurements by drifters from 2001 to 2017, from the Bank of Oceanographic Data of Marine Hydrophysical Institute.

(B) Temperature and salinity measured by deepsea buoy–profilers at horizons from 4 to 1500 m (565 profiles for 2005–2008).

(C) Monthly averages of nighttime satellite measurements of SST at a 4×4 km grid for 1985–2007 [7].

Hydrological fields were constructed on the basis of the data grouped over decades with a five–year overlap. Combining the data over the decades ensured their uniform spatial distribution on most horizons, which allowed horizontal interpolation. An array of temperature and salinity climate data of the Black Sea contains 12 files with mean monthly fields. Each file consists of thirty–six 141×88 arrays. The data is available at the following depths: 0, 10, 20, 30, 40, 50, 75, 100, 120, 150, 200, 300, 500, 600, 800, 1000, 1200, 1500, 1800, 2000 m. Horizontal longitudinal resolution was $1/10^\circ$, latitudinal— $1/16^\circ$ in the region of 27.8° – 41.8° E, 40.875° – 46.3125° W. Temperature and salinity data were selected for each of the 18 transects, shown at Fig. 1, for 4 months, from May to August

(144 files). The seawater density (ρ , $\text{kg}\cdot\text{m}^3$) was calculated from the International Equation of State (UNESCO) [8]. Profiles of buoyancy frequency $N(z)$ defined as $N^2(z) = -\frac{g}{\rho(z)} \frac{\partial \rho(z)}{\partial z}$ were estimated for all density profiles. Here, $\rho(z)$ is the density, z is the vertical coordinate (positive upward), and g is the acceleration due to gravity. Both $\rho(z)$ and $N(z)$ profiles were gridded to bins of the vertical axis

4.2 The Equations of Propagation of Internal Waves

The phenomenon of wave transformation caused by bottom variation is explained theoretically using nonlinear equations for shallow water waves. Internal waves can propagate along the interface of two homogeneous layers or in a continuously stratified fluid. We considered a rotated basin of variable depth filled with stratified water at the latitude of 44°N . The linearized equations of motion under the Boussinesq approximation are as follows

$$\rho \left(\frac{\partial u}{\partial t} - fv \right) = -\frac{\partial P}{\partial x}, \quad \rho \left(\frac{\partial v}{\partial t} + fu \right) = -\frac{\partial P}{\partial y}, \quad \rho \frac{\partial w}{\partial t} + \rho' g = -\frac{\partial P}{\partial z}, \quad (1)$$

$$\frac{\partial u}{\partial x} + \frac{\partial v}{\partial y} + \frac{\partial w}{\partial z} = 0,$$

where where $\rho'(z)$ is the background density perturbation; P is the pressure; u , v , and w are the velocity components along the standard orthogonal coordinates x , y , and z , respectively;—is offshore distance coordinate; $f = 1.01 \cdot 10^{-4} \text{ s}^{-1}$ —is the Coriolis parameter. For internal waves propagating along the bottom, the governing system (1) can be reduced to one equation for the vertical velocity component $w = W(z)\exp[i(kx + \omega t)]$, where k is the wavenumber along the horizontal plane, ω —is the wave frequency, and $W(z)$ satisfies:

$$\frac{\partial^2 W}{\partial^2 z} + k^2 \left(\frac{N^2(z) - f^2}{\omega^2 - f^2} - 1 \right) = 0. \quad (2)$$

with the following boundary conditions

$$W(0) = W(H) = 0, \quad (3)$$

where H is the water depth. Using the dispersion relation $\omega^2 = C^2 k^2 + f^2$, (2) can be rewritten as $\frac{\partial^2 W}{\partial^2 z} + \left(\frac{N^2(z) - f^2}{C^2} \right) W = k^2 W$. Approximating the derivatives with the finite differences discretized over Δz yields a standard form of eigenvalue problem. The internal waves dispersion characteristics and the normal mode vertical profiles were estimated by solving numerically the following boundary value problem [6]:

$$\frac{\partial^2 W}{\partial^2 z} + \left(\frac{N^2(z) - \omega^2}{C_{in}^2} \right) W = 0, \quad \text{where } C_{in}^2 = \frac{\omega^2 - f^2}{k_n^2} \quad (4)$$

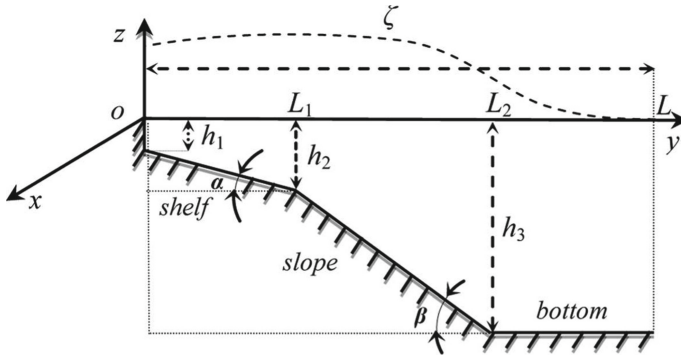


Fig. 3. Model geometry profile.

with the boundary conditions (3). Here, C_i refers to the internal wave phase speed in a nonrotating ocean, and $n = 1, 2, \dots$ is the vertical mode number.

In our study we used the topography of the Black Sea from the *GEBCO* database (<http://www.gebco.net>). It has a spatial resolution for the longitude with 0.008334°E step, latitude with 0.008342°N step. The topography of the continental shelf and slope is approximated as a two-slope depth profile adjacent to a deep ocean of a constant depth. The parameters of the transects in the considered region depend only on one spatial variable (Fig. 3).

The depth profile is characterized by the width of the shelf, slope, and deep ocean (L_1 and L_2) as well as by the depth of the coastal wall, shelf break, and deep ocean (h_1 , h_2 and h_3). Table 1 contains the parameters of some bottom shape profiles; rows for each profile indicate the depth values at the shore (h_1), slope (h_2), and offshore (h_3) and the width values of the shelf (L_1), and continental slope (L_2). It also shows the inclination angle for the shelf (α) and slope (β).

Table 1. Profiles geometry.

| Profiles | Shelf | | | Slope | | | Bottom |
|----------|-----------|------------|----------------|-----------|------------|---------------|-----------|
| | h_1 , m | L_1 , km | α , deg | h_2 , m | L_2 , km | β , deg | h_3 , m |
| 1 | 2 | 75,2 | 32 | 158 | 16,0 | 45 | 1685 |
| 10 | 11 | 46,2 | 38 | 189 | 27,7 | 44 | 1331 |
| 12 | 74 | 33,4 | 34 | 158 | 17,6 | 45 | 1831 |
| 18 | 22 | 25,0 | 39 | 146 | 14,9 | 45 | 1419 |

Shelf of the Crimean coast is quite wide (profiles 1–4) reaching 67.3–79 km in width. A sharp transition to the continental slope (where the maximum $\alpha = 45$) is observed at profile 5. Profiles 13–18 are the most special, where the shelf is very narrow (L_1 is 23.3–28.2 km), the bottom inclinations are small, and $h(y)$ profile is close to the quasi-linear one.

4.3 Observations of Internal Waves Near the Black Sea Coast of the Crimea

The available Sentinel-2 and Landsat-8 data for 2016–2017 were analyzed. Images of satisfactory quality (cloudiness less than 30%) were selected. Internal waves appeared only at 6 images for 2016 (out of 32) and at 25 images for 2017 (out of 53). Thus the period from May to September, 2017 was selected for the analysis. The following operations were performed with the selected images:

(A) Preparation of composite images with enhanced contrast.

(B) Localization of internal waves appearance, separation from ship-generated waves.

(C) Obtaining georeferenced perimeter of 6 anchor points for each wave (3 frontal and 3 rear).

(D) Saving the waves parameters (front width, wavelength, number of waves in packet, direction, date and time).

After that, the results were visualized with QGIS 2.18 and statistically analyzed with MS Excel.

5 Results and Discussion

5.1 Analysis of Buoyancy Frequency Profiles

The water stratification profile (constructed as initial conditions for numerical experiments) was characterized by a relatively sharp interface at the depth of 50 m and a less pronounced main pycnocline located between 500 and 1200 m deep (see Fig. 4). The vertical distribution of buoyancy frequency in spring and summer is different (left vs central panel). In the summer, the $N(z)$ curves differ little in different parts of the coast

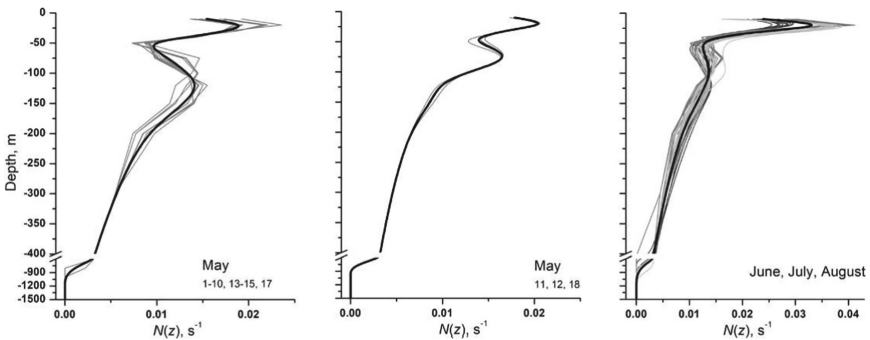


Fig. 4. Vertical profiles of buoyancy frequency $N(z)$. In the left and central panels, lines correspond to the transects (1–10, 13–15, 17) and (11, 12, 18), respectively, during the spring. In the right panel lines correspond to the transects 1–18 during the summer. Black lines show the averaged $N(z)$.

5.2 Theoretical Estimate of the Fundamental Mode Parameters

For the interpretation of observations, we calculate wave properties (Table 2) and eigenvectors for the vertical velocity component $W(z)$ of baroclinic Poincaré waves in the ocean of depth H described by equation (4).

Figure 5 shows the results of calculation of volume waves maps for three offshore profiles. Calculations were made for seasonally different buoyancy frequency profiles—late spring and summer. Spatial distribution of the vertical velocity of the first mode waves was analyzed using the maps in Fig. 5, left panel. Significant vertical movement of water was found in the deep sea in spring, and in the area of the sharp continental slope in summer, which was caused by a more powerful flow of the Rim current jet at the edge of the shelf. At the shelf with a sharper slope ($\alpha = 45^\circ$), the maximum vertical velocity for both zones was found in the deep sea. In profile 10 one can see that in summer internal waves appear above the edge of the shelf and propagate in both directions from the disturbances sources.

Table 2. Parameters of the three main baroclinic modes in the central part of Kalamita Bay for the spring profile of $N(z)$.

| Mode | Wavelength, m | Phase speed, ms^{-1} | Period, h |
|---------------------------------|---------------|-------------------------------|-----------|
| Deep part, maximum depth 1500 m | | | |
| 1 | 2416 | 0.93 | 7.21 |
| 2 | 950 | 0.35 | 5.86 |
| 3 | 459 | 0.27 | 4.51 |
| Shelf part, maximum depth 300 m | | | |
| 1 | 770 | 0.58 | 0.37 |
| 2 | 290 | 0.25 | 0.32 |
| 3 | 210 | 0.18 | 0.32 |

The highest vertical velocities for the second mode wave (Fig. 5, central panel) take place in the surface layer. The zero-amplitude curve, running at a depth of 150–300 m, lies almost horizontally in spring, and bends to the bottom in summer (profiles 12, 17). Maps of the third mode vertical wave velocity distribution (Fig. 5, right panel) confirm the influence of bottom topography on their structure. The position of the first nodal line of the third mode is much closer to the sea surface (50–200 m) in comparison with the zero amplitude curve of the second mode and largely repeats its shape.

The second nodal line is located at a depth of 400–800 m and in the summer it usually repeats the configuration of the steep slope (profiles 10, 17) or sometime differs from the shape of the first nodal line (profile 12). The highest values of the velocity of the third mode waves occur in the surface (100–200 m) and deep (800–1200 m) layers of the sea. For the deep part of the slope the phase velocity

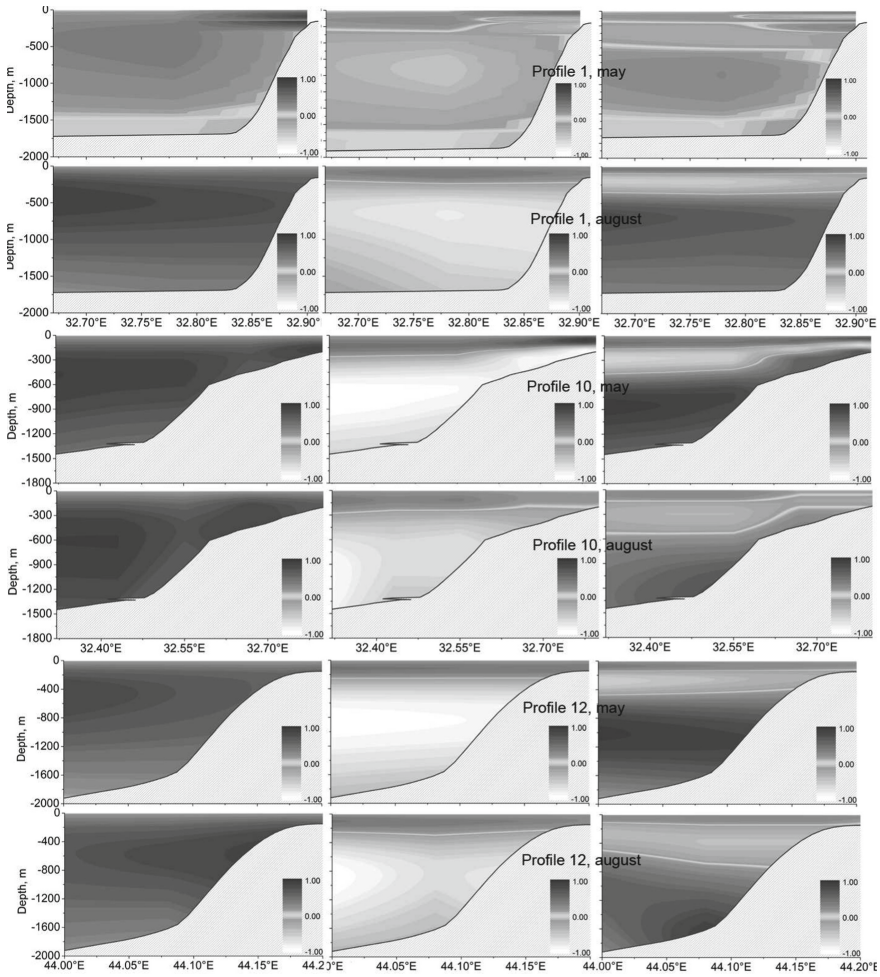


Fig. 5. Volume waves maps for the vertical velocity field $W(z)$ along the profiles 1, 10 and 12. Results of numerical experiment for a spring and summer buoyancy frequency of $N(z)$: 1 mode (left), 2 mode (center) and 3 mode (right).

of the internal waves of the first mode at the given profiles varies from 2.6 to 5 ms^{-1} (C) depending on the season, their length from 9 to 180 km (λ); for the waves of the second mode— 1.1 – 2.3 ms^{-1} (C), 4 – 42 km (λ); for the waves of the third mode— 0.7 – 1.4 ms^{-1} (C), 1 – 27 km (λ).

5.3 Comparison of Model Calculations with Satellite Observations

Qualitative analysis of the maps of waves distribution and direction showed that the areas of the most recent waves appearance were located to the North–West of the Heracles Peninsula (where the quasi–steady Sevastopol anticyclone is known

to be formed) and to the North–East of it, in the shallow Kalamita bay. The waves detected over the wide shelf oriented mainly shoreward and those found at the slope—along the shelf.

129 cases of internal waves propagation were identified from May to September, 2017. The distribution over the months is not equal. In June, 50 waves were observed, which is the highest number, while in May and September only 12 and 6 respectively. From July to August the number of waves decreased from 42 to 19. Wavelengths varied from 0.05 to 1.14 km with a mean value of 0.4 km and a median value very close to it: 0.375 km. Thus most waves were 0.15 km to 0.6 km long. The longest waves, around 0.8 km, were more often observed between Sevastopol and Yevpatoria along the 50 m isobaths.

6 Conclusion

The main spatial and temporal characteristics of internal waves at the shelf of the Crimean coast were determined on the basis of satellite sensing data and the results of analytical calculations. The assumed reason for generation of intense internal waves through the interaction of the Rim current jet with the shelf edge was confirmed by the results of numerical calculations of the vertical distribution of the first three modes velocity. The mathematical modeling allowed us to obtain theoretical estimates of the parameters of internal waves depending on the season and shape of the longshore relief. Comparing the wavelengths of the observed and calculated waves, we can conclude that during 2017 the waves of 2 and 3 modes were observed from the satellite in the area of study the most frequently. They propagate up to 1200 m deep and typically manifest themselves the most intensively at the distance 20–30 km from the coast, depending on the shelf width and vertical water density profile.

Acknowledgments. The reported study was funded by RFBR and Government of Sevastopol according to the research project No 18–45–920036. The authors thank Professor Aleksander E. Yankovsky (University of South Carolina) for supporting this research and consultations in creating the applications for processing information on the intra–wave oscillations.

References

1. Ivanov, V.A., Konyaev, K.V., Serebryanyy, A.N.: Groups of intensive internal waves on the sea shelf. *Izvestiya AN SSSR Fizika atmosfery i okeana* **17**(12), 1302–1309 (1981)
2. Klimov, D.M., Karev, V.I., Kovalenko, Y.F., Ustinov, K.B.: Mechanical-mathematical and experimental modeling of well stability in anisotropic media. *Mech. Solids* **48**, 357–363 (2013)
3. Ivanov, V.A., Serebryanyy, A.N.: Short-period internal waves in the coastal zone of a non-tidal sea. *Izvestiya AN SSSR Atmos. Ocean. Phys.* **21**(6), 648–656 (1985)
4. Colosi, J.A., Beardsley, R.C., Lynch, J.F.: Observations of nonlinear internal waves on the outer New England continental shelf during summer Shelfbreak Primer study. *Geophys. Res.* **106**(C5), 9587–9601 (2001)

5. Liu, A.K., Chang, Y.S., Hsu, M.K., Liang, N.K.: Evolution of nonlinear internal waves in the East and South China Seas. *Geophys. Res.* **103**(C4), 7995–8008 (1998)
6. Yankovsky, A.E., Zhang, T.: Scattering of a semidiurnal barotropic kelvin wave into in-ternal waves over wide continental shelves dynamics. *Phys. Ocean.* **47**, 2745–2762 (2017)
7. Polonsky, A.B., Shokurova, I.G., Belokopytov, V.N.: Decadal temperature and salinity fields at standard levels in the Black Sea. *Phys. Ocean.* **6**, 27–41 (2013)
8. Algorithms for computation of fundamental properties of seawater. UNESCO technical papers in marine science, vol. 44, p. 53. UNESCO (1983)